Scilight

Complex Systems Stability & Control
https://www.sciltp.com/journals/cssc

Article

Predefined-Time Fault-Tolerant Consensus Tracking Control for Multiple Flexible Robotic Manipulator Systems with Prescribed Performance

Chaowen He [1], Alain Martinez [2], Ben Niu [3], Deepak Kumar Jain [3], Yuqiang Jiang [1,*], Dmytro Zubov [4], Yuanxin Li [5] and Xiaomei Wang [6,*]

[1] School of Electrical Engineering, Sichuan University, Chengdu 610065, China
[2] Faculty of Electrical Engineering, Central University Marta Abreu of Las Villas, Santa Clara 50100, Cuba
[3] Key Laboratory of Intelligent Control and Optimization for Industrial Equipment of Ministry of Education, School of Control Science and Engineering, Dalian University of Technology, Dalian 116024, China
[4] Department of Computer Science, University of Central Asia, Naryn 722900, Kyrgyzstan
[5] College of Science, Liaoning University of Technology, Jinzhou 121001, China
[6] School of Automation, Chongqing University, Chongqing 400044, China
* Correspondence: jiangyuqiang721@163.com (Y.J.); wlwxmei@163.com (X.W.)

How To Cite: He, C.; Martinez, A.; Niu, B.; et al. Predefined-Time Fault-Tolerant Consensus Tracking Control for Multiple Flexible Robotic Manipulator Systems with Prescribed Performance. *Complex Systems Stability & Control* **2025**, *1*(1), 7.

Received: 28 August 2025
Revised: 12 November 2025
Accepted: 18 November 2025
Published: 26 November 2025

Abstract: This article focuses on the predefined-time fault-tolerant consensus tracking control problem for the multiple single-link flexible robotic manipulator systems (FRMSs) with prescribed performance. Firstly, a predefined time performance function is provided to ensure the tracking error of the flexible robotic manipulator system (FRMS) reaches a predefined accuracy within a predefined time. Second, a new error coordinate system replaces the original control system to constrain the consensus control errors between the leader and the follower of the multiple FRMSs maintain the area set by the user. Thirdly, considering that the actuators of the multiple FRMSs are vulnerable to faults during long periods of operation, an adaptive compensation mechanism is proposed to improve the FRMS's fault tolerance. Lastly, simulation results validate the effectiveness of the control scheme.

Keywords: multiple flexible robotic manipulator systems; predefined-time; prescribed performance; fault-tolerant

1. Introduction

The FRMS can replace human labor in dangerous and mechanized tasks, which gives it a wide range of applications in both civilian [1] and military [2] fields. Facing complex environments in different fields, the FRMS is required to accomplish control goals with faster response, higher accuracy, and stronger robustness. Therefore, finite-time control (FTC) [3] was proposed to achieve these control objectives. Along the way of thinking, researchers have made many outstanding results [4–10]. For example, a finite-time event-triggered control strategy was developed for the FRMS in [4] to reduce the communication burden while achieving finite-time convergence. Ref. [5] proposed a low-cost neuroadaptive control scheme for the FRMS that avoids signal singularities while achieving finite-time convergence. Ref. [8] presented a finite-time output regulation method for the FRMS with input delays, which allowed the position tracking error converge to a small region near zero in finite-time. However, the FTC is related to the initial state, limiting its development. For this reason, the concept of fixed-time control (FxTC) was introduced in [11]. The advantage of FxTC over FTC is that the convergence time does not depend on the initial state, which is completely determined by the control parameters. Based on this work [11], researchers have achieved many accomplishments [12–16]. As an illustration, Ref. [12] combined fractional-order sliding mode controller with fixed-time theory to achieve FxTC of the FRMS with uncertain disturbances. Ref. [14] proposed a fixed-time composite anti-disturbance control for n-degrees-of-freedom the FRMS, which ensured that the system's output tracked time-varying

output tracked time-varying trajectories while realizing the suppression of elastic vibrations. However, the FxTC's convergence time has a complex relationship with the control parameters, and the convergence time cannot be set directly. To fill this gap, the predefined time control (PTC) [17] is proposed. Along this line of study [17], researchers have achieved a lot of results [18–22]. Compared with the traditional backstepping method, the predefined-time composite fuzzy adaptive control scheme that was proposed in [18] significantly reduces the computational burden and improves operational efficiency. Ref. [19] proposed a practical adaptive predefined-time neural control method for the FRMS with uncertain joint dynamics and input saturation. Although the aforementioned results exhibit satisfactory convergence time, practical applications such as welding require not only rapid convergence but also stringent constraints on the tracking error [23]. Therefore, achieving fast convergence while constraining the tracking error within strict bounds has become a prominent research focus.

Prescribed performance control (PPC) [24–29] utilizes a prescribed performance function in the controller, enabling the tracking error to be maintained within a specified range. Ref. [24] designed a prescribed performance controller based on backstepping and robust adaptive control for the rigid-flexible coupled manipulator, which can constrain the tracking error under input quantization. Ref. [25] proposed a fuzzy adaptive control strategy that integrates a prescribed performance function with an event-triggered mechanism, thereby ensuring tracking accuracy and reducing the communication burden. In [27], an adaptive prescribed performance controller was designed for a robotic system with model uncertainty, external disturbances, and actuator saturation to achieve finite-time tracking control with prescribed performance. However, the productivity efficiency of a single system is finite, and real-world production often requires the cooperation of multiple systems.

As a key technique in cooperative control, consensus control has yielded numerous research results [30–33]. Ref. [30] employed reinforcement learning algorithms to tackle the consensus control of nonlinear multi-agent systems with actuator efficiency loss and time-varying bias faults. Ref. [31] proposed a consensus control strategy under undirected graphs, addressing the problem of consensus control and vibration suppression in nonlinear Timoshenko manipulators. Although many aspects of the FRMS consensus control have been considered in previous studies, enabling multiple robots to achieve a prescribed performance within a predefined time remains a worthwhile research topic with significant implications for practical production. Furthermore, actuator failure is an unavoidable challenge that has always been considered in previous works [28,34,35].

Based on the above discussion, this paper aims to study a predefined-time fault-tolerant consensus tracking control approach for the multiple FRMSs with prescribed performance. The proposed consensus control scheme ensured that the output error of all the FRMS satisfies the prescribed transient and steady-state performance specifications. Our contribution, which differs from existing studies, is summarized as follows:

(1) Unlike existing predefined-time control methods [26,27] where convergence time is inherently dependent on initial system states or tedious control parameter tuning, our proposed controller decouples convergence time from these factors—it can be directly preset by the user according to specific application requirements. Meanwhile, compared with prior prescribed performance or predefined-time schemes [18–20] our design ensures that tracking errors strictly remain within the user-defined bounded region throughout the entire control process, achieving both predictable convergence speed and precise error control.

(2) A distributed control strategy is proposed for the multiple FRMSs with unknown uncertainties. Compared with the results in [29], this design not only addresses the scalability issue but also ensures that the output can be linearly or even superlinearly enhanced by simply adding more FRMSs—without requiring reconfiguration of the core control algorithm or sacrificing control performance.

(3) In practical engineering, the actuators of the FRMSs are vulnerable to faults in hostile working environments. An adaptive compensation mechanism is proposed for the multiple FRMSs, which can achieve high-precision trajectory tracking and improve the FRMSs' fault tolerance. Rigorous Lyapunov analysis confirms that all follower FRMSs can still reach consensus with the leader under actuator faults, and the consensus error is strictly bounded within the user-prescribed region—filling the gap between practical fault resilience and precise performance guarantees.

The framework of this paper is as follows. Section II introduces the preliminaries work. Section III presents controller design and stability analysis. Next, Section IV discusses the simulation study. Finally, Section V final conclusion of the work.

2. Preliminaries

2.1. Graph Knowledge

Every FRMS is regarded as a node. The communication relationships among FRMSs are described by a directed graph $G = (E, N_d)$ represent the direct topology graph of N agents, where $E = \{e_1, \ldots, e_N\}$ is a group of nodes and $N_d \subseteq E \times E$ is a group of edges. The edge $(e_i, e_j) \in E$ denotes that the ith agent can receive the

data from its neighboring the jth agent. The followers' adjacency matrix is defined as $A = [a_{i,j}] \in \mathbb{R}^{N\times N}$, which represents the relationship of followers in G. If the ith agent can receive the data from its neighbors, then $a_{i,j} > 0$, and otherwise $a_{i,j} = 0$. The followers' in-degree matrix is selected as $D = diag\{\sum_{j=1}^{N} a_{1,j}, \ldots, \sum_{j=1}^{N} a_{N,j}\}$. The followers' Laplacian matrix is chosen as $L = D - A$. The graph G only has one leader, which can only send data to its neighboring followers. Thus, the leader's adjacency matrix is chosen as $B = diag\{b_{1,0}, \ldots, b_{N,0}\}$.

2.2. Actuator Fault Model

Actuator faults [36–38] are common problems in practical control systems. Consider specifically intermittent actuator faults as follows:

$$\begin{cases} U_i(t) = \rho_i u_i(t), \\ t^s \le t < t^e, \end{cases} \tag{1}$$

where U_i denotes the actual output, and u_i denotes the expected output. Moreover, the efficiency factor $\rho_i \in (0, 1]$ of the actuator is an unknown constant. Specifically, if $\rho_i = 1$, the actuator functions normally; otherwise, it undergoes partial loss of effectiveness (PLOE). The fault initiation and termination times are denoted as t^s and t^e, respectively.

2.3. Predefined-Time Prescribed Performance Transformation

An error transformation mechanism is provided to ensure that the tracking errors between the FRMSs and the leader achieve the predefined accuracy within the predefined time.

A predefined-time performance function [39] is defined as follows:

$$p(t) = \begin{cases} (p_0 - p_{T_s})e^{\frac{\gamma_k t}{t - T_s}} + p_{T_s}, & t \in [0, T_s), \\ p_{T_s}, & t \in [T_s, +\infty), \end{cases} \tag{2}$$

where T_s represents the predefined settling time. p_0 and p_{T_s} are positive constants and they satisfy the relationship $p_0 > p_{T_s}$. The term γ_k is a positive constant. For $\forall t \ge 0$, $p(t)$ satisfies $p(t) > 0$. The natural constant is expressed by e, and $p(t)$ is abbreviated as p.

2.4. System Description

Consider the single-link FRMS integrated with both robotic and actuator dynamics. The dynamic model derived from the Euler-Lagrangian formulation is formulated as follows:

$$\begin{aligned} \mathrm{M}(q)\ddot{q} + C(q, \dot{q})\dot{q} + G(q) + F(\dot{q}) &= K(q_m - q), \\ J\ddot{q}_m + B\dot{q}_m + K(q_m - q) &= U, \end{aligned} \tag{3}$$

where the position, velocity and acceleration vectors of the link are denoted by $q, \dot{q}, \ddot{q} \in \mathbb{R}$, respectively. The rotor angular position, velocity and acceleration vectors are denoted by $q_m, \dot{q}_m, \ddot{q}_m \in \mathbb{R}$, respectively. $M(q) \in \mathbb{R}$ is the inertia matrix, $C(q, \dot{q}) \in \mathbb{R}$ is the Coriolis and centripetal forces, $G(q) \in \mathbb{R}$ is the gravity vector, and $F(\dot{q}) \in \mathbb{R}$ represents the friction term. The positive definite diagonal matrices $K, J, B \in \mathbb{R}$, represent the joint flexibility, actuator inertia, and natural damping term, respectively. $U \in \mathbb{R}^n$ is the torque input at each actuator. The structure diagram is shown in Figure 1.

By defining the state variables $x_1 = q$, $x_2 = \dot{q}$, $x_3 = q_m$, $x_4 = \dot{q}_m$, the system (1) can be transformed as

$$\begin{cases} \dot{x}_1 = x_2, \\ \dot{x}_2 = K_M x_3 + f_2(\bar{x}_2), \\ \dot{x}_3 = x_4, \\ \dot{x}_4 = J^{-1}U + f_4(\bar{x}_4), \\ y = x_1, \end{cases} \tag{4}$$

where $K_M = K/M(x_1)$, $f_2(\bar{x}_2) = (1/M(x_1))\ (-C(x_1, x_2)x_2 - G(x_1) - F(x_2) - Kx_1)$, $\bar{x}_2 = \{x_1, x_2\}$,

$f_4(\bar{x}_4) = (1/J)(-Bx_4 - K(x_3 - x_1))$, $\bar{x}_4 = \{x_1, x_2, x_3, x_4\}$. So for the ith follower, its equations are given by

$$\begin{cases} \dot{x}_{i,1} = x_{i,2}, \\ \dot{x}_{i,2} = K_M x_{i,3} + f_{i,2}(\bar{x}_{i,2}), \\ \dot{x}_{i,3} = x_{i,4}, \\ \dot{x}_{i,4} = J^{-1}U_i + f_{i,4}(\bar{x}_{i,4}), \\ y_i = x_{i,1}, \end{cases} \tag{5}$$

where $K_M = K/M(x_{i,1})$, $f_{i,2}(\bar{x}_{i,2}) = (1/M(x_{i,1}))(-C(x_{i,1}, x_{i,2})x_{i,2} - G(x_{i,1}) - F(x_{i,2}) - Kx_{i,1})$, $\bar{x}_{i,2} = \{x_{i,1}, x_{i,2}\}$, $f_{i,4}(\bar{x}_{i,4}) = (1/J)\left(-Bx_{i,4} - K(x_{i,3} - x_{i,1})\right)$, $\bar{x}_{i,4} = \{x_{i,1}, x_{i,2}, x_{i,3}, x_{i,4}\}$.

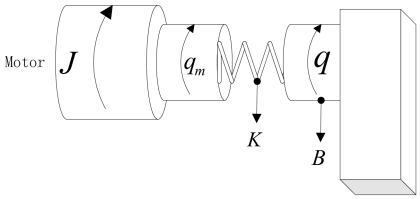

Figure 1. Structure diagram.

2.5. Assumptions and Lemmas

Assumption 1. *The desired signal y_d and $\dot{y}_d$ are both bounded and known smooth functions.*

Lemma 1. ***[40]:*** *Let $f(x)$ be a continuous function on a compact set Ω. Then for any scalar $\varepsilon > 0$, there exists a fuzzy logic system (FLS) such that*

$$\sup_{x \in \Omega} \left| f(x) - w^T \varphi(x) \right| \leq \varepsilon, \tag{6}$$

where $w = [w_1, \ldots, w_M]^T$ is the ideal constant weight vector and $\varphi(x) = [p_1(x), p_2(x), \ldots, p_M(x)]^T / \sum_{i=1}^{N} p_i(x)$ is the basic function vector with $M > 1$ being the number of the fuzzy rules. p_i is chosen as Gaussian function, i.e., for $\forall i = 1, 2, \ldots, M$, $p_i(x) = \exp[\frac{-(x-\mu_i)^T(x-\mu_i)}{\gamma_i^2}]$, where $\mu_i = [\mu_{i1}, \ldots, \mu_{im}]^T$ is the center vector and γ_i is the width of the Gaussian function.

Lemma 2. ***[41]:*** *The positive constant ε satisfies the following inequality:*

$$0 \leq |x| - \frac{x^2}{\sqrt{x^2 + \varepsilon^2}} \leq \varepsilon, \tag{7}$$

where $x \in \mathbb{R}$ is an arbitrary constant.

Lemma 3. ***[42]:*** *If the graph G contains a spanning tree and the leader node is the root node, then all eigenvalues of $H = L + B$ are positive real parts.*

Lemma 4. ***[39]:*** *The vector $\boldsymbol{E}$ and $\boldsymbol{B}$ satisfy*

$$\mathbf{E}^T\mathbf{F} \leq \frac{\underline{\kappa}\mathbf{E}^T\mathbf{E}}{2} + \frac{\mathbf{F}^T\mathbf{F}}{2\underline{\kappa}}, \tag{8}$$

where $\underline{\kappa}$ is a positive constant.

Lemma 5. ***[43]:*** *Define $z_1 = (z_{1,1}, z_{2,1}, \ldots, z_{N,1})^T$, $y = (y_1, y_2, \ldots, y_N)^T$, $\underline{y}_d = (y_d, y_d, \ldots, y_d)^T$, then*

$$\left\| y - \underline{y}_d \right\| \leq \|z_1\| / \underline{\sigma}(L + B),$$

where $\underline{\sigma}(L + B)$ is the minimum singular value of $L + B$.

3. Main Result

3.1. Controller Design

The following paragraphs provide a detailed demonstration of the controller design process illustrated in Figure 2.

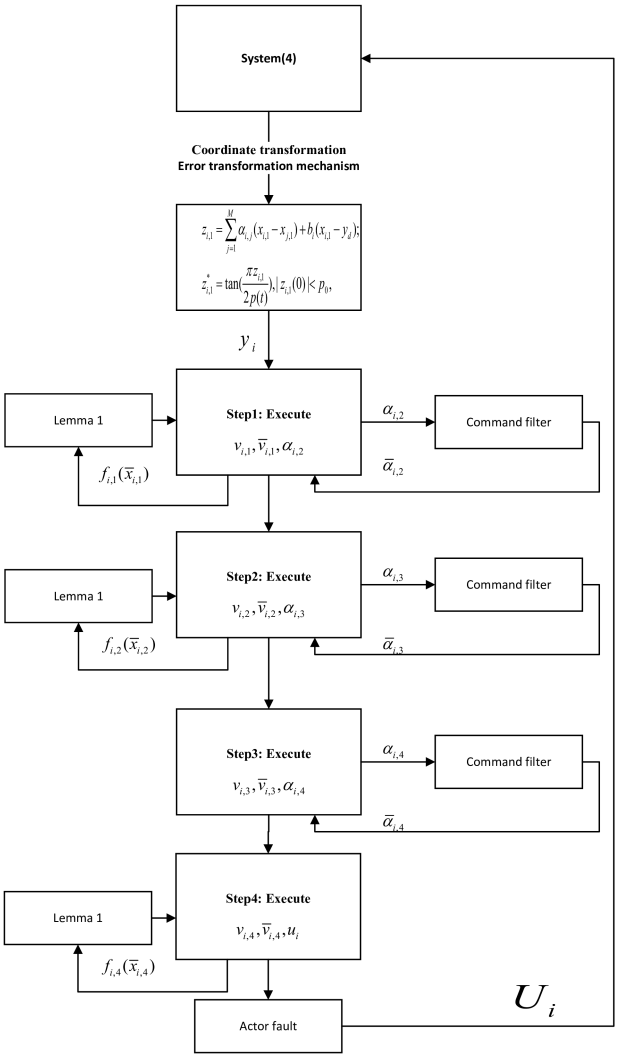

Figure 2. Block diagram of the backstepping design.

The consensus tracking error for the ith FRMS is represented as

$$z_{i,1} = \sum_{j}^{M} a_{i,j}(x_{i,1} - x_{j,1}) + b_i(x_{i,1} - y_d), \tag{9}$$

where y_d represents the desired trajectory signal.

The performance Equation (2) is used for the following error transformation mechanism:

$$z_{i,1}^* = \tan(\frac{\pi z_{i,1}}{2p(t)}), |z_{i,1}(0)| < p_0, \tag{10}$$

where z_{i1}^* is the consensus tracking error after transformation. The derivative of z_{i1}^* is calculated as

$$\begin{aligned} \dot{z}_{i,1}^* = Q_{i,1}\Big(d_i x_{i,2} - \sum_{j=1}^{M} a_{i,j} x_{j,2} - b_i \dot{y}_d \\ - \frac{2\dot{p}(t)}{\pi} \arctan(z_{i,1}^*)\Big), \end{aligned} \tag{11}$$

and the $Q_{i,1} = \frac{\pi(1+z_{i,1}^{*\,2})}{2p(t)}$, $d_i = \sum_{j=1}^{M} a_{i,j} + b_i$.

The coordinate transformation based on first-order filter is defined as follows:

$$\begin{cases} v_{i,1} = z_{i,1}^*, \\ v_{i,s} = x_{i,s} - \bar{\alpha}_{i,s}, s = \{2,3,4\}, \end{cases} \tag{12}$$

$$\varpi_{i,s}\dot{\bar{\alpha}}_{i,s} + \bar{\alpha}_{i,s} = \alpha_{i,s}, s = \{2,3,4\}, \tag{13}$$

where $\bar{\alpha}_{i,s}$ is the output of the first-order command filter. Additionally, the input–output relationship of the filter [29] is illustrated in (13). $\varpi_{i,s}$ is a designed positive parameter, and α_{is} stands for the input of the filter.

Define the error after compensation as follows:

$$\bar{v}_{i,s} = v_{i,s} - \eta_{i,s}, s = \{1,2,3,4\}, \tag{14}$$

where $\bar{v}_{i,s}$ is the error after compensation, and the term η_{is} is a subsequently designed compensation signal.

The following paragraphs provide the controller design process.

Step 1: The Lyapunov function $\bar{V}_{i,1}$ is constructed as follows:

$$\bar{V}_{i,1} = \frac{1}{2}\bar{v}_{i,1}^2 + \frac{\tilde{\theta}_{i,1}^2}{2\varepsilon_{i,1}}, \tag{15}$$

where, $\tilde{\theta}_{i1} = \theta_{i1} - \hat{\theta}_{i1}$ denotes the adaptive estimated error. And $\theta_{is} \triangleq \max\{\|w_{ik}\|^2\}$, $i = 1,\ldots,N, k = 1,\ldots,M, s = 1,\ldots,4$, w_{ik} is the ideal weight vectors of the FLS. The estimated value of θ_{i1} is represented by the term $\hat{\theta}_{i1}$, and the term ε_{i1} is a positive parameter.

The derivative of $\bar{V}_{i,1}$ is calculated as

$$\begin{aligned} \dot{\bar{V}}_{i,1} =& \bar{v}_{i,1}[Q_{i,1}(d_i(v_{i,2} + \bar{\alpha}_{i,2} - \alpha_{i,2} + \alpha_{i,2}) \\ & - \sum_{j=1}^{N} a_{i,j}x_{j,2} - b_i\dot{y}_d - \frac{2\dot{p}}{\pi}\arctan(z_{i,1}^*)) \\ & - \dot{\eta}_{i,1}] - \frac{1}{\varepsilon_{i,1}}\tilde{\theta}_{i,1}\dot{\hat{\theta}}_{i,1}. \end{aligned} \tag{16}$$

Define an unknown function $f_{i1}(X_{i,1}) = -\sum_{j=1}^{N} a_{i,j}x_{j,2}$, and $X_{i,1} = [x_{j,2}]^T$.The upper boundary of $\sigma_{i,1}$ is expressed as $\sigma_{i,1}^*$. According to Lemma 1 and Lemma 4, we obtain

$$\begin{aligned} \bar{v}_{i,1}Q_i f_{i,1}(X_{i,1}) =& \bar{v}_{i,1}Q_{i,1}[w_{i,1}^T\varphi_{i,1}(X_{i,1}) + \sigma_{i,1}] \\ \leq& \frac{\bar{v}_{i,1}^2}{2}Q_{i,1}^2\theta_{i1}||\varphi(X_{i,1})||^2 \\ & + \frac{1}{2} + \frac{\bar{v}_{i,1}^2}{2}Q_{i,1}^2 + \frac{\sigma^{*\,2}_{i,1}}{2}. \end{aligned} \tag{17}$$

The compensation signal $\eta_{i,1}$ is designed as

$$\begin{aligned} \dot{\eta}_{i,1} =& -c_{i,1}\eta_{i,1} + Q_{i,1}d_i(\bar{\alpha}_{i,2} - \alpha_{i,2} + \eta_{i,2}) \\ & - h_{i,1}Q_{i,1}^2 d_i\eta_{i,1}, \end{aligned} \tag{18}$$

where c_{i1} and h_{i1} are positive constants.

Using Lemma 4 again

$$\bar{v}_{i,1}h_{i,1}Q_{i,1}^2 d_i\eta_{i,1} \leq \frac{d_i^2Q_{i,1}^4\bar{v}_{i,1}^2\eta_{i,1}^2}{2} + \frac{h_{i,1}^2}{2}. \tag{19}$$

Combining (16)–(19), we design $\alpha_{i,2}$ as

$$\begin{aligned} \alpha_{i,2} =& -\frac{c_{i,1}v_{i,1}}{d_iQ_{i,1}} + \frac{1}{d_i}(\frac{2\dot{p}}{\pi}\arctan(z_{i,1}^*) \\ & - \frac{Q_{i,1}\bar{v}_{i,1}}{2} + b_i\dot{y}_d - \frac{\bar{v}_{i,1}}{2}Q_{i,1}\hat{\theta}_{i,1}||\varphi(X_{i,1})||^2 \\ & - \frac{d_i^2\bar{v}_{i,1}\eta_{i,1}^2Q_{i,1}^3}{2}). \end{aligned} \tag{20}$$

By plugging (18) and (20) into (16), we have

$$\begin{aligned}\dot{\bar{V}}_{i,1} \leq & -c_{i,1}\bar{v}_{i,1}^2 + Q_{i,1}d_i\bar{v}_{i,1}\bar{v}_{i,2} \\ & + \tilde{\theta}_{i,1}\left(\frac{\bar{v}_{i,1}^2 Q_{i,1}||\varphi(X_{i,1})||^2}{2} - \frac{\dot{\hat{\theta}}_{i,1}}{\varepsilon_{i,1}}\right) \\ & + \frac{1+\sigma^{*2}_{i,1}+h_{i,1}^2}{2}.\end{aligned} \tag{21}$$

The adaptive law $\hat{\theta}_{i,1}$ is defined as follows:

$$\dot{\hat{\theta}}_{i,1} = -\bar{\varepsilon}_{i,1}\hat{\theta}_{i,1} + \frac{\bar{v}_{i,1}^2 Q_{i,1}^2||\varphi(X_{i,1})||^2\varepsilon_{i,1}}{2}, \tag{22}$$

where $\bar{\varepsilon}_{i,1}$ is a positive design parameter.

Substituting (22) into (21) yields

$$\dot{\bar{V}} \leq -c_{i,1}\bar{v}_{i,1}^2 + Q_{i,1}d_i\bar{v}_{i,1}\bar{v}_{i,2} + \phi_{i,1} + \frac{\bar{\varepsilon}_{i,1}}{\varepsilon_{i,1}}\tilde{\theta}_{i,1}\hat{\theta}_{i,1}, \tag{23}$$

with $\phi_{i,1} = \frac{1+\sigma^{*2}_{i,1}+h_{i,1}^2}{2}$.

Step 2: The Lyapunov function $\bar{V}_{i,2}$ is constructed as follows:

$$\bar{V}_{i,2} = \bar{V}_{i,1} + \frac{1}{2}\bar{v}_{i,2}^2 + \frac{1}{2\varepsilon_{i,2}}\tilde{\theta}_{i,2}^2, \tag{24}$$

where, $\tilde{\theta}_{i2} = \theta_{i2} - \hat{\theta}_{i2}$ denotes the adaptive estimated error. The estimated value of θ_{i2} is represented by the term $\hat{\theta}_{i2}$, and the term ε_{i2} is a positive parameter.

Then we can attain

$$\begin{aligned}\dot{\bar{V}}_{i,2} = & \dot{\bar{V}}_{i,1} + \bar{v}_{i,2}(K_M(v_{i,3} + \bar{\alpha}_{i,3} - \alpha_{i,3} + \alpha_{i,3}) \\ & + f_{i,2}(\bar{x}_{i,2}) - \dot{\bar{\alpha}}_{i,2} - \dot{\eta}_{i,2}) - \frac{1}{\varepsilon_{i,2}}\tilde{\theta}_{i,2}\dot{\hat{\theta}}_{i,2},\end{aligned} \tag{25}$$

Based on Lemma 4, we obtain

$$\begin{aligned}\bar{v}_{i,2}f(\bar{x}_{i,2}) = & \bar{v}_{i,2}[w_{i,2}^T\varphi_{i,2} + \sigma_{i,2}] \\ \leq & \frac{1}{2}\bar{v}_{i,2}^2\theta_{i,2}||\varphi_{i,2}||^2 \\ & + \frac{1}{2} + \frac{1}{2}\bar{v}_{i,2}^2 + \frac{{\sigma^*_{i,2}}^2}{2},\end{aligned} \tag{26}$$

where $\sigma^*_{i,2}$ stands for the upper boundary of $\sigma_{i,2}$.

The compensation signal $\eta_{i,2}$ is designed as

$$\begin{aligned}\dot{\eta}_{i,2} = & -c_{i,2}\eta_{i,2} + K_M(\bar{\alpha}_{i,3} - \alpha_{i,3}) \\ & + K_M\eta_{i,3} - Q_{i,1}d_i\eta_{i,1}.\end{aligned} \tag{27}$$

From (25) to (27), we get

$$\begin{aligned}\dot{\bar{V}}_{i,2} \leq & \dot{\bar{V}}_{i,1} + \bar{v}_{i,2}(K_M\bar{v}_{i,3} + K_M\alpha_{i,3} \\ & + \frac{1}{2}\bar{v}_{i,2}\theta_{i,2}||\varphi_{i,2}||^2 + \frac{1}{2}\bar{v}_{i,2} - \dot{\bar{\alpha}}_{i,2} \\ & + c_{i,2}\eta_{i,2} + Q_{i,1}d_i\eta_{i,1}) + \phi_{i,2} - \frac{1}{\varepsilon_{i,2}}\tilde{\theta}_{i,2}\dot{\hat{\theta}}_{i,2},\end{aligned} \tag{28}$$

with $\phi_{i,2} = \frac{1}{2} + \frac{{\sigma^*_{i,2}}^2}{2}$. The virtual controller $\alpha_{i,3}$ is designed as

$$\begin{aligned}\alpha_{i,3} =& \frac{1}{K_M}(-\frac{\bar{v}_{i,2}}{2}\hat{\theta}_{i,2}||\varphi(X_{i,2})||^2 \\ & - c_{i,2}v_{i,2} - Q_i d_i v_{i,1} + \dot{\bar{\alpha}} - \frac{1}{2}v_{i,2}).\end{aligned} \tag{29}$$

Substituting (29) into (28) we obtain

$$\begin{aligned}\dot{\bar{V}}_{i,2} \leq & \dot{\bar{V}}_{i,1} + \bar{v}_{i,2}(K_M\bar{v}_{i,3} - c_{i,2}\bar{v}_{i,2} - Q_{i,1}d_i\bar{v}_{i,1}) \\ & + \tilde{\theta}_{i,2}(\frac{\bar{v}^2_{i,2}}{2}||\varphi(\bar{x}_{i,2})||^2 - \frac{\dot{\hat{\theta}}_{i2}}{\varepsilon_{i,2}}) + \phi_{i,2}.\end{aligned} \tag{30}$$

The adaptive law $\hat{\theta}_{i,2}$ is designed as

$$\dot{\hat{\theta}}_{i,2} = -\bar{\varepsilon}_{i,2}\hat{\theta}_{i,2} + \frac{\varepsilon_{i,2}}{2}\bar{v}^2_{i,2}||\varphi(\bar{x}_{i,2})||^2, \tag{31}$$

where $\bar{\varepsilon}_{i,2}$ is a positive design parameter.

By plugging (31) and (23) into (30), we have

$$\begin{aligned}\dot{\bar{V}}_{i,2} \leq & - c_{i,1}\bar{v}^2_{i,1} - c_{i,2}\bar{v}^2_{i,2} + K_M\bar{v}_{i,2}\bar{v}_{i,3} \\ & + \frac{\bar{\varepsilon}_{i,1}}{\varepsilon_{i,1}}\tilde{\theta}_{i,1}\hat{\theta}_{i,1} + \frac{\bar{\varepsilon}_{i,2}}{\varepsilon_{i,2}}\tilde{\theta}_{i,2}\hat{\theta}_{i,2} + \phi_{i,1} + \phi_{i,2}.\end{aligned} \tag{32}$$

Step 3: The Lyapunov function $\bar{V}_{i,3}$ is constructed as follows:

$$\bar{V}_{i,3} = \bar{V}_{i,2} + \frac{1}{2}\bar{v}^2_{i,3}. \tag{33}$$

Then, we attain

$$\begin{aligned}\dot{\bar{V}}_{i,3} =& \dot{\bar{V}}_{i,2} + \bar{v}_{i,3}(v_{i,4} + \bar{\alpha}_{i,4} \\ & - \alpha_{i,4} + \alpha_{i,4} - \dot{\bar{\alpha}}_{i,3} - \dot{\eta}_{i,3}).\end{aligned} \tag{34}$$

The compensation signal $\eta_{i,3}$ is designed as

$$\dot{\eta}_{i,3} = -c_{i,3}\eta_{i,3} - K_M\eta_{i,2} + \eta_{i,4} + (\bar{\alpha}_{i,4} - \alpha_{i,4}). \tag{35}$$

Designing the controller $\alpha_{i,4}$ as

$$\alpha_{i,4} = -c_{i,3}v_{i,3} - K_M v_{i,2} + \dot{\bar{\alpha}}_{i,3}. \tag{36}$$

Combining (32)–(36), we obtain

$$\begin{aligned}\dot{\bar{V}}_{i,3} = & - c_{i,1}\bar{v}^2_{i,1} - c_{i,2}\bar{v}^2_{i,2} - c_{i,3}\bar{v}^2_{i,3} + \bar{v}_{i,3}\bar{v}_{i,4} \\ & + \phi_{i,1} + \phi_{i,2} + \frac{\bar{\varepsilon}_{i,1}}{\varepsilon_{i,1}}\tilde{\theta}_{i,1}\hat{\theta}_{i,1} + \frac{\bar{\varepsilon}_{i,2}}{\varepsilon_{i,2}}\tilde{\theta}_{i,2}\hat{\theta}_{i,2}.\end{aligned} \tag{37}$$

Step 4: Define $l_i = J^{-1}$, $\omega_{i4} = \inf_{t\geq 0}\{l_i\rho_i\}$ with $i \in [1, N]$. Due to the facts $0 < \rho_i \leq 1$ and $l_i > 0$, we obtain $\omega_{i4} > 0$. Moreover, further define $\Omega_{ib} = \min\{\omega_{i4}\}$ and $\delta_{ib} = 1/\Omega_{ib}$.

Then, the Lyapunov function $\bar{V}_{i,4}$ is designed as follows:

$$\bar{V}_{i,4} = \bar{V}_{i,3} + \frac{1}{2}\bar{v}^2_{i,4} + \frac{1}{2\varepsilon_{i,4}}\tilde{\theta}^2_{i,4} + \frac{\Omega_{i,b}}{2\varepsilon_{i,b}}\tilde{\delta}^2_i. \tag{38}$$

where, $\tilde{\theta}_{i4} = \theta_{i4} - \hat{\theta}_{i4}$ denotes the adaptive estimated error. The estimated value of θ_{i4} is represented by the term $\hat{\theta}_{i4}$. $\tilde{\delta}_{ib} = \delta_{ib} - \hat{\delta}_{ib}$ is the relevant estimated error. And the term ε_{i4}, ε_{ib} are positive parameters.

Then, we attain

$$\begin{aligned}\dot{\bar{V}}_{i,4} =&\dot{\bar{V}}_{i,3} + \bar{v}_{i,4}(\frac{1}{J}\rho_i u_i + f_{i,4}(\bar{x}_{i,4}) - \dot{\bar{\alpha}}_{i,4} - \dot{\eta}_{i,4}) \\ &- \frac{1}{\varepsilon_{i,4}}\tilde{\theta}_{i,4}\dot{\hat{\theta}}_{i,4} - \frac{\Omega_{i,b}}{\varepsilon_{i,b}}\tilde{\delta}_{i,b}\dot{\hat{\delta}}_{i,b}.\end{aligned} \tag{39}$$

Based on Lemmas 1 and 4, we obtain

$$\begin{aligned}\bar{v}_{i,4}f_{i,4}(\bar{x}_{i,4}) =&\bar{v}_{i,4}[w_{i,4}^T\varphi_{i,4} + \sigma_{i,4}] \\ \leq&+ \frac{1}{2}\bar{v}_{i,4}\theta_{i,4}||\varphi(\bar{x}_{i,4})||^2 + \frac{1}{2} \\ &+ \frac{1}{2}\bar{v}_{i,4}^2 + \frac{1}{2}{\sigma_{i,4}^*}^2.\end{aligned} \tag{40}$$

Substituting (40) into (39), we get

$$\begin{aligned}\dot{\bar{V}}_{\mathrm{i4}} \leq&\dot{\bar{V}}_{\mathrm{i3}} + \bar{v}_{i,4}(\frac{1}{J}\rho_i u_i + \frac{1}{2}\bar{v}_{i,4}\theta_{i,4}||\varphi(\bar{x}_{i,4})||^2 \\ &+ \frac{1}{2}v_{i,4} + \mu_i - \mu_i - \dot{\bar{\alpha}}_{i,4} - \dot{\eta}_{i,4}) \\ &+ \phi_{i,4} - \frac{1}{\varepsilon_{i,4}}\tilde{\theta}_{i,4}\dot{\hat{\theta}}_{i,4} - \frac{\Omega_{i,b}}{\varepsilon_{i,b}}\tilde{\delta}_{i,b}\dot{\hat{\delta}}_{i,b},\end{aligned} \tag{41}$$

where $\phi_{i,4} = \frac{1}{2} + \frac{1}{2}{\sigma_{i,4}^*}^2$, μ_i represents the intermediate control law.

Designing μ_i as follows:

$$\begin{aligned}\mu_i =&c_{i,4}v_{i,4} + v_{i,3} + \frac{1}{2}\bar{v}_{i,4}\hat{\theta}_{i,4}||\varphi(\bar{x}_{i,4})||^2 \\ &+ \frac{1}{2}v_{i,4} - \dot{\bar{\alpha}}_{\mathrm{i4}},\end{aligned} \tag{42}$$

The compensation signal $\eta_{i,4}$ is designed as

$$\dot{\eta}_{i,4} = -c_{i,4}\eta_{i,4} - \eta_{i,3}, \tag{43}$$

The controller u_i is designed as

$$u_i = -\frac{\bar{v}_{i,4}\hat{\delta}_{i,b}^2\mu_i^2}{\sqrt{\bar{v}_{i,4}^2\hat{\delta}_{i,b}\mu_i^2 + \varepsilon_{i,u}^2}}, \tag{44}$$

where $\varepsilon_{i,u}$ is a designed constant.

Based on Lemma 2, we can obtain:

$$\begin{aligned}\bar{v}_{i,4}\frac{1}{J}\rho_i u_i \leq&\frac{\Omega_{i,b}\bar{v}_{i,4}^2\hat{\delta}_{i,b}^2\mu_i^2}{\sqrt{\bar{v}_{i,4}^2\hat{\delta}_{i,b}\mu_i^2 + \varepsilon_{i,u}^2}} \\ \leq&-\Omega_{i,b}\bar{v}_{i,4}\hat{\delta}_{i,b}\mu_i + \Omega_{i,b}\varepsilon_{i,b},\end{aligned} \tag{45}$$

The term $-\Omega_{i,b}\bar{v}_{i,4}\hat{\delta}_{i,b}\mu_i$ satisfies the following equation:

$$\begin{aligned}-\Omega_{i,b}\bar{v}_{i,4}\hat{\delta}_{i,b}\mu_i =&-\Omega_{i,b}\bar{v}_{i,4}\delta_{i,b}\mu_i + \Omega_{i,b}\bar{v}_{i,4}\tilde{\delta}_{i,b}\mu_i \\ =&-\bar{v}_{i,4}\mu_i + \Omega_{i,b}\bar{v}_{i,4}\tilde{\delta}_{i,b}\mu_i.\end{aligned} \tag{46}$$

Combining (41)–(46), we get

$$\begin{aligned}\dot{\bar{V}}_{i,4} \leq&\dot{\bar{V}}_{i,3} - c_{i,4}\bar{v}_{i,4}^2 - \bar{v}_{i,3}\bar{v}_{i,4} + \tilde{\theta}_{i,4}(\frac{\bar{v}_{i,4}^2}{2}||\varphi(\bar{x}_{i,4})||^2 \\ &- \frac{\dot{\hat{\theta}}_{i,4}}{\varepsilon_{i,4}}) + \Omega_{i,b}\tilde{\delta}_{i,b}(\bar{v}_{i,4}\mu_i - \frac{\dot{\hat{\delta}}_{i,b}}{\varepsilon_{i,b}}),\end{aligned} \tag{47}$$

The adaptive laws are designed as follows:

$$\dot{\hat{\theta}}_{i,4} = -\bar{\varepsilon}_{i,4}\hat{\theta}_{i,4} + \frac{\varepsilon_{i,4}}{2}\bar{v}_{i,4}^2||\varphi(\bar{x}_{i,4})||^2, \tag{48}$$

$$\dot{\hat{\delta}}_{i,b} = -\bar{\varepsilon}_{i,b}\hat{\delta}_{i,b} + \varepsilon_{i,b}\bar{v}_{i,4}\mu_i, \tag{49}$$

where $\bar{\varepsilon}_{i,4}$ and $\bar{\varepsilon}_{i,b}$ are the positive design parameters. Substituting (37), (48), and (49) into (47), we obtain

$$\begin{aligned}\dot{\bar{V}}_{i,4} \leq & -c_{i,1}\bar{v}_{i,1}^2 - c_{i,2}\bar{v}_{i,2}^2 - c_{i,3}\bar{v}_{i,3}^2 - c_{i,4}\bar{v}_{i,4}^2 \\ & + \phi_{i,1} + \phi_{i,2} + \phi_{i,4} + \frac{\bar{\varepsilon}_{i,1}}{\varepsilon_{i,1}}\tilde{\theta}_{i,1}\hat{\theta}_{i,1} \\ & + \frac{\bar{\varepsilon}_{i,2}}{\varepsilon_{i,2}}\tilde{\theta}_{i,2}\hat{\theta}_{i,2} + \frac{\bar{\varepsilon}_{i,4}}{\varepsilon_{i,4}}\tilde{\theta}_{i,4}\hat{\theta}_{i,4} + \frac{\Omega_{i,b}\bar{\varepsilon}_{i,b}}{\varepsilon_{i,b}}\tilde{\delta}_{i,b}\hat{\delta}_{i,b},\end{aligned} \tag{50}$$

According to Lemma 4, we have

$$\begin{cases} \frac{\bar{\varepsilon}_{i,1}}{\varepsilon_{i,1}}\tilde{\theta}_{i,1}\hat{\theta}_{i,1} \leq \frac{\bar{\varepsilon}_{i,1}}{2\varepsilon_{i,1}}\theta_{i,1}^2 - \frac{\bar{\varepsilon}_{i,1}}{2\varepsilon_{i,1}}\tilde{\theta}_{i,1}^2, \\ \frac{\bar{\varepsilon}_{i,2}}{\varepsilon_{i,2}}\tilde{\theta}_{i,2}\hat{\theta}_{i,2} \leq \frac{\bar{\varepsilon}_{i,2}}{2\varepsilon_{i,2}}\theta_{i,2}^2 - \frac{\bar{\varepsilon}_{i,2}}{2\varepsilon_{i,2}}\tilde{\theta}_{i,2}^2, \\ \frac{\bar{\varepsilon}_{i,4}}{\varepsilon_{i,4}}\tilde{\theta}_{i,4}\hat{\theta}_{i,4} \leq \frac{\bar{\varepsilon}_{i,4}}{2\varepsilon_{i,4}}\theta_{i,4}^2 - \frac{\bar{\varepsilon}_{i,4}}{2\varepsilon_{i,4}}\tilde{\theta}_{i,4}^2, \\ \frac{\Omega_{i,b}\bar{\varepsilon}_{i,b}}{\varepsilon_{i,b}}\tilde{\delta}_{i,b}\hat{\delta}_{i,b} \leq \frac{\Omega_{i,b}\bar{\varepsilon}_{i,b}}{2\varepsilon_{i,b}}\delta_{i,b}^2 - \frac{\Omega_{i,b}\bar{\varepsilon}_{i,b}}{2\varepsilon_{i,b}}\tilde{\delta}_{i,b}^2. \end{cases} \tag{51}$$

Combining (50) and (51), we have

$$\begin{aligned}\dot{\bar{V}}_{i,4} \leq & -\sum_{s=1}^{4}(c_{i,s}\bar{v}_{i,s}^2) + \phi_{i,1} + \phi_{i,2} + \phi_{i,4} + \frac{\bar{\varepsilon}_{i,1}}{2\varepsilon_{i,1}}\theta_{i,1}^2 \\ & - \frac{\bar{\varepsilon}_{i,1}}{2\varepsilon_{i,1}}\tilde{\theta}_{i,1}^2 + \frac{\bar{\varepsilon}_{i,2}}{2\varepsilon_{i,2}}\theta_{i,2}^2 - \frac{\bar{\varepsilon}_{i,2}}{2\varepsilon_{i,2}}\tilde{\theta}_{i,2}^2 + \frac{\bar{\varepsilon}_{i,4}}{2\varepsilon_{i,4}}\theta_{i,4}^2 \\ & - \frac{\bar{\varepsilon}_{i,4}}{2\varepsilon_{i,4}}\tilde{\theta}_{i,4}^2 + \frac{\Omega_{i,b}\bar{\varepsilon}_{i,b}}{2\varepsilon_{i,b}}\delta_{i,b}^2 - \frac{\Omega_{i,b}\bar{\varepsilon}_{i,b}}{2\varepsilon_{i,b}}\tilde{\delta}_{i,b}^2.\end{aligned} \tag{52}$$

3.2. Stability Analysis

The following theorem summarizes the above work.

Theorem 1. *For multiple FRMSs* (5) *under Assumption 1, Lemma 1 to 5, the compensation signals* (18), (27), (35), *and* (43), *the adaptive laws* (22), (31), (48), (49), *the virtual controllers* (20), (29), (36), *and the controller* (44), *the explored control scheme can achieve the following:*

1. *The consensus errors of the FRMSs can achieve the predetermined accuracy within the pre-defined time.*
2. *All signals within the closed-loop system are bounded.*

Proof. The Lyapunov function of compensation signals is constructed as

$$\bar{V}_{i,\eta} = \frac{1}{2}\sum_{s=1}^{4}\eta_{i,s}^2. \tag{53}$$

According to (18), (27), (35), and (43), we can attain

$$\begin{aligned}\dot{\bar{V}}_{i,\eta} = & -\sum_{s=1}^{4}c_{i,s}\eta_{i,s}^2 + Q_{i,1}d_i(\bar{\alpha}_{i,2} - \alpha_{i,2})\eta_{i,1} \\ & - h_{i,1}Q_{i,1}^2 d_i\eta_{i,1}^2 + K_M(\bar{\alpha}_{i,3} - \alpha_{i,3})\eta_{i,2} \\ & + (\bar{\alpha}_{i,4} - \alpha_{i,4})\eta_{i,3}.\end{aligned} \tag{54}$$

Based on [44], we can conclude that $||\bar{\alpha}_{i,s} - \alpha_{i,s}|| \leq \ell_{i,s}(\ell_{i,s} > 0)$, $\ell_{i,s}$ is a known constant. So (54) can be rewritten as

$$\begin{aligned}\dot{\bar{V}}_{i,\eta} = & -\sum_{s=1}^{4}c_{i,s}\eta_{i,s}^2 + Q_{i,1}d_i\ell_{i,2}\eta_{i,1} - h_{i,1}Q_{i,1}^2 d_i\eta_{i,1}^2 \\ & + K_M\ell_{i,3}\eta_{i,2} + \ell_{i,4}\eta_{i,3}.\end{aligned} \tag{55}$$

By Lemma 4 we have

$$\begin{cases} Q_{i,1}d_i\ell_{i,2}\eta_{i,1} \leq \frac{d_i m Q_{i,1}^2\eta_{i,1}^2}{2} + \frac{d_i\ell_{i,2}^2}{2m}, \\ K_M\ell_{i,3}\eta_{i,2} \leq \frac{\eta_{i,2}^2}{2} + \frac{{K_M}^2\ell_{i,3}^2}{2}, \\ \ell_{i,4}\eta_{i,3} \leq \frac{\eta_{i,3}^2}{2} + \frac{\ell_{i,4}^2}{2}. \end{cases} \tag{56}$$

where m is a design parameter.

Combining (56) and (55), we get

$$\begin{aligned} \dot{\bar{V}}_{i,\eta} \leq & -c_{i,1}\eta_{i,1}^2 - (h_{i,1} - \frac{m}{2})Q_{i,1}^2\eta_{i,1}^2 d_i - (c_{i,2} - \frac{1}{2})\eta_{i,2}^2 \\ & - (c_{i,3} - \frac{1}{2})\eta_{i,3}^2 - c_{i,4}\eta_{i,4}^2 + \phi_{i,\eta}, \end{aligned} \tag{57}$$

where $\phi_{i,\eta} = \frac{d_i\ell_{i,2}^2}{2m} + \frac{{K_M}^2\ell_{i,3}^2}{2} + \frac{\ell_{i,4}^2}{2}$.

Designing the constants h_{i1} to satisfy the condition $h_{i1} \geq 1/2$, one yields

$$\begin{aligned} \dot{\bar{V}}_{i,\eta} \leq & -c_{i,1}\eta_{i,1}^2 - (c_{i,2} - \frac{1}{2})\eta_{i,2}^2 - (c_{i,3} - \frac{1}{2})\eta_{i,3}^2 \\ & - c_{i,4}\eta_{i,4}^2 + \phi_{i,\eta}, \\ \leq & -c_{i,\eta}\bar{V}_{i,\eta} + \phi_{i,\eta}, \end{aligned} \tag{58}$$

where $c_{i,\eta} = \min\{2c_{i,1}, 2(c_{i,2} - \frac{1}{2}), 2(c_{i,3} - \frac{1}{2}), 2c_{i,4}\}$. According to Liapunov's stability theorem, it can be obtained that the error of the compensation signals is bounded.

For all FRMSs, the total Lyapunov function can be expressed as

$$\bar{V}_F = \sum_{i=1}^{N}(\bar{V}_{i,4} + \bar{V}_{i,\eta}). \tag{59}$$

According to (50) and (57), it can be obtained that the derivative of $\bar{V}_F$ satisfies the following inequality:

$$\dot{\bar{V}}_F \leq -a_F\bar{V}_F + b_F, \tag{60}$$

where $a_F = \min\{2c_{i,1}, 2(c_{i,2} - \frac{1}{2}), 2(c_{i,3} - \frac{1}{2}), 2c_{i,4}, \bar{\varepsilon}_{i,1}, \bar{\varepsilon}_{i,2}, \bar{\varepsilon}_{i,4}, \bar{\varepsilon}_{i,b}\}$, $b_F = \sum_{i=1}^{N}(\phi_{i,1}+\phi_{i,2} + \phi_{i,4} + \phi_{i,\eta} + \frac{\bar{\varepsilon}_{i,1}}{2\varepsilon_{i,1}}\theta_{i,1}^2 + \frac{\bar{\varepsilon}_{i,2}}{2\varepsilon_{i,2}}\theta_{i,2}^2 + \frac{\bar{\varepsilon}_{i,4}}{2\varepsilon_{i,4}}\theta_{i,4}^2 + \frac{\Omega_{i,b}\bar{\varepsilon}_{i,b}}{2\varepsilon_{i,b}}\delta_{i,b}^2)$.

By integrating inequality (60) over the interval $[0, t]$, it can be derived that

$$0 \leq \bar{V}_F \leq (\bar{V}_F(0) - \frac{b_F}{a_F})e^{-a_F t} + \frac{b_F}{a_F}, \forall t \in [0, +\infty) \tag{61}$$

which means that signals $\bar{v}_{i,s}$, η_{is}, $\tilde{\theta}_{i1}$, $\tilde{\theta}_{i3}$, $\tilde{\theta}_{i4}$, $\tilde{\delta}_{ib}$, $s = \{1, 2, 3, 4\}$, $i = \{1, \ldots, N\}$, of system (5) are bounded.

Since $\bar{v}_{i,s} = v_{i,s} - \eta_{i,s}$, it is easy to obtain that the signal $v_{i,s}$ is also bounded. Based on (10) and (12) we can further get

$$-p(t) \leq z_{i,1}(t) \leq p(t), t \in [0, +\infty), \tag{62}$$

when $t \in [T_s, +\infty)$

$$-p_{T_s} \leq z_{i,1}(t) \leq p_{T_s}, t \in [T_s, +\infty). \tag{63}$$

Which means that by designing a suitable p_{T_s}, the consensus errors can be limited to a predefined accuracy in a predefined time.

Defining the consensus errors vector as $z_{i,1} = [z_{1,1}, z_{2,1}, \ldots, z_{N,1}]^T$, the tracking errors vector as $e_1 = [y_1 - y_d, y_2 - y_d, \ldots, y_N - y_d]^T$. According to Lemma 5 we obtain

$$||e_1|| \leq \frac{||z_{i,1}||}{H} < \frac{\sqrt{N}P(t)}{H}, t \in [0, +\infty). \tag{64}$$

Based on (64) one can further obtain

$$|y_i - y_d| < \frac{\sqrt{N}P(t)}{H}, t \in [0, +\infty). \tag{65}$$

And (65) can be rewritten as

$$-\frac{\sqrt{N}P(t)}{H} < y_i - y_d < \frac{\sqrt{N}P(t)}{H}, t \in [0, +\infty). \tag{66}$$

Combining (2) and (66), when $t \in [T_s, +\infty)$, we get

$$-\frac{\sqrt{N}p_{T_s}}{H} < y_i - y_d < \frac{\sqrt{N}p_{T_s}}{H}, t \in [T_s, +\infty). \tag{67}$$

What this implies is that the positive constant p_{T_s} being selected, the tracking errors can meet the predetermined accuracy within the predefined time T_s. □

Remark 1. *In the controller design process, numerous adaptive laws (such as $\hat{\theta}_{i,1}, \hat{\theta}_{i,2}, \hat{\theta}_{i,4}, \hat{\delta}_{i,b}$,) require online updates. The fuzzy approximation of unknown nonlinear function $w^T\varphi(x)$ involves multiplication operations. Compared with [45], the introduction of the first-order filter $\varpi_{i,s}\dot{\bar{\alpha}}_{i,s} + \bar{\alpha}_{i,s} = \alpha_{i,s}$ alleviates the burden of derivative computation—each filter only requires a small number of floating-point operations per time step, contributing minimally to the overall complexity. The nonlinear error transformation (10) and compensation signals ($\eta_{i,1}, \eta_{i,2}, \eta_{i,3}, \eta_{i,4}$.) involve algebraic operations and the solution of derivatives of performance functions, but due to the adoption of closed-form expressions, they offer high computational efficiency.*

4. Simulation Study

The FRMS is widely used in automated factories, and the consensus control of multiple robotic manipulator systems has a significant effect on improving productivity.

Considering the ith single-link robotic manipulator from [46] shown in Figure 1, and the dynamic model can be obtained

$$\begin{cases} ml^2\ddot{q}_i + mgl\sin(q_i) + \cos(\dot{q}_i) = K(q_{i,m} - q_i), \\ J\ddot{q}_{m,i} + B\dot{q}_{m,i} + K(q_{m,i} - q_i) = U_i, \\ y = q_i, \end{cases} \tag{68}$$

where $q, \dot{q}, \ddot{q}, q_m, \dot{q}_m, \ddot{q}_m \in \mathbb{R}$, $m = 0.5$ kg, $l = 0.75$ m, $g = 9.8$ m/s^2, $K = 140$ N·m/rad, $J = 0.35$ kg·m^2, and $B = 0.95$. The communication topology of the multi-FRMSs is shown in Figure 3. Ten FRMSs are considered to simultaneously process the same batch of products in a limited space. To ensure consistent product quality, the FRMS must coordinate to achieve a specified tracking accuracy within a predefined time.

The design parameters are chosen as: $p_0 = 1, p_{Ts} = 0.3, m = 0.001, T_s = 2, \varepsilon_{i,u} = 0.005, \gamma_k = 0.4, h_{i,1} = 0.001, c_{i1} = 5, c_{i2} = 15, c_{i3} = 5, c_{i4} = 15, \varepsilon_{i1} = 10, \varepsilon_{i2} = 10, \varepsilon_{i4} = 10, \varepsilon_{ib} = 10, \bar{\varepsilon}_{ib} = 0.1, \bar{\varepsilon}_{i1} = 0.1, \bar{\varepsilon}_{i2} = 0.1, \bar{\varepsilon}_{i4} = 0.1, \varpi_{i,2} = 0.01, \varpi_{i,3} = 0.01, \varpi_{i,4} = 50, i = 1, ..., 9, t^s = 3, t^e = 8, \rho_i = 0.5$. Setting the initial value as $x_{11} = 0.5, x_{21} = 0.4, x_{31} = 0.3$, the remaining initial values are set to 0.1. The desired signal is $y_d = \sin(t)$.

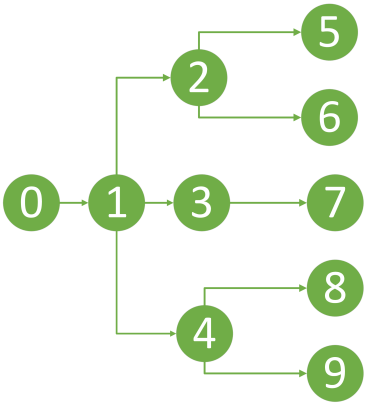

Figure 3. Communication topology of the multiple FRMSs.

The simulation results under the communication topology shown in Figure 3 are displayed in Figures 4–6. It can be clearly seen from Figure 4 that, under the control method proposed in this paper, all the FRMSs are capable of converging to the preset control accuracy within 2 s. In Figure 5 $z_{i,1} = y_i - y_d$ demonstrates the relationship between the tracking errors and the preset accuracy, and it can be seen that all the errors are within the preset

accuracy. As shown in Figure 6, the actuators of the FRMS fails within 3–8 s, resulting in only 50% of the desired control signal. It can be observed that, under the control method proposed in this paper, a robust control tracking performance is still achieved even when partial actuator failures occur. As shown in Figure 7, compared with the finite-time method in [6], this paper not only achieves convergence within a preset time but also realizes the coordinated control of multiple flexible robotic manipulator systems.

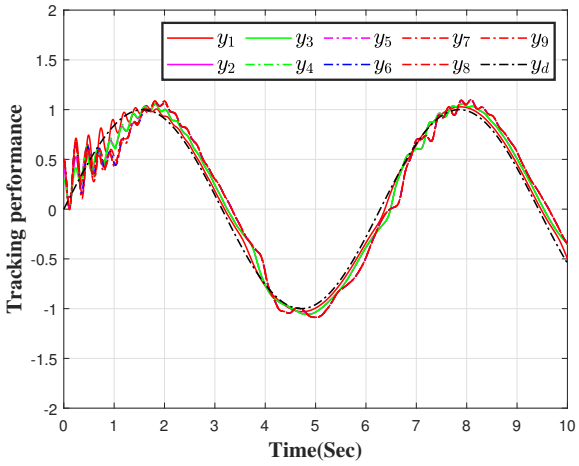

Figure 4. Output trajectories of three followers and the leader.

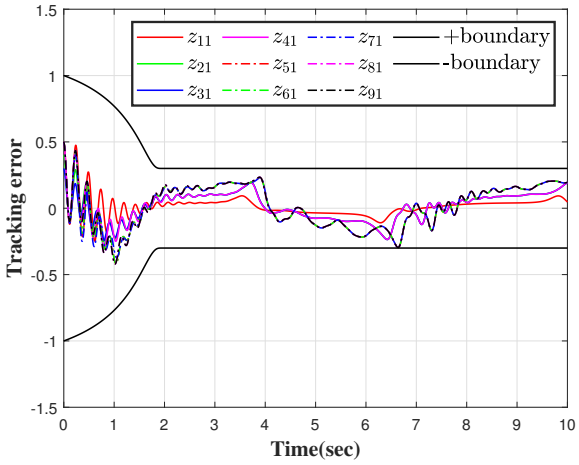

Figure 5. Output errors of three followers and the leader.

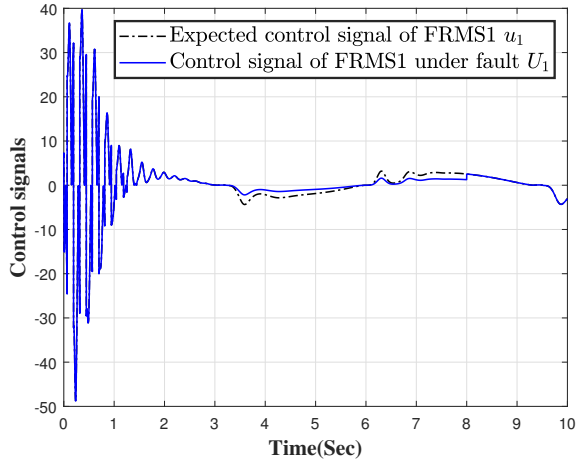

Figure 6. The control input of FRMS1.

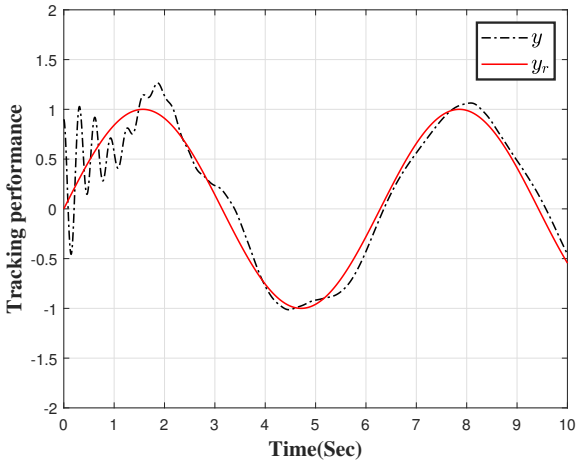

Figure 7. Adapted with permission from Ref. [6]. Copyright 2023, Xiaomei Wang.

5. Conclusions

This paper investigated the predefined-time fault-tolerant control problem for the multiple FRMSs with prescribed performance constraints. First, a predefined-time function was used to control the convergence time of the system, which can be set by the user. Second, a new error coordinate system replaced the original control system to constrain the consensus control errors between the leader and the follower of the multiple FRMSs maintain the area set by the user. Second, a distributed control strategy was employed, which addressed the scalability of the multiple FRMSs. Third, an adaptive compensation mechanism was proposed for the multiple FRMSs, which can achieve high-precision trajectory tracking and improve the FRMS's fault tolerance. Finally, the simulation result was carried out to demonstrate the validity of the designed algorithm. Next, efforts will focus on PTC-based adaptive control for FRMS, dealing with the cyber attacks and complex environmental conditions.

Author Contributions

C.H.: data curation, writing—original draft preparation; A.M., B.N., D.K.J., D.Z., Y.L. and X.W.: supervision; Y.J.: writing—reviewing and editing. All authors have read and agreed to the published version of the manuscript.

Funding

This research was funded in part by the National Natural Science Foundation of China (Nos. U25A20455, 62376170, 62506052), in part by the in part the Natural Science Foundation of Liaoning Province of China (No. 2025-MS- 013), in part by the Natural Science Foundation of Chongqing of China (No. CSTB2025NSCQ-GPX0746), in part by China Postdoctoral Science Foundation (No. 2025M771718), and in part by Postdoctoral Fellowship Program of China Postdoctoral Science Foundation (No. GZC20251189).

Institutional Review Board Statement

Not applicable.

Informed Consent Statement

Not applicable.

Data Availability Statement

Not applicable.

Conflicts of Interest

The authors declare no conflict of interest.

Use of AI and AI-Assisted Technologies

No AI tools were utilized for this paper.

References

1. Qiao, H.; Wu, Y.X.; Zhong, S.L.; et al. Brain-inspired intelligent robotics: Theoretical analysis and systematic application. *Mach. Intell. Res.* **2023**, *20*, 1–18.
2. Liu, Y.; Chen, Z.; Gao, J.; et al. High performance assembly of complex structural parts in special environments–research on space manipulator assisted module docking method. *Robot. Intell. Autom.* **2023**, *43*, 122–131.
3. Bhat, S.P.; Bernstein, D.S. Finite-time stability of continuous autonomous systems. *SIAM J. Control. Optim.* **2000**, *38*, 751–766.
4. Feng, Y.; Kong, L.; Zhang, Z.; et al. Event-triggered finite-time control for a constrained robotic manipulator with flexible joints. *Int. J. Robust Nonlinear Control.* **2023**, *33*, 6031–6051.
5. Zhou, B.; Yang, L.; Wang, C.; et al. Adaptive finite-time tracking control of robot manipulators with multiple uncertainties based on a low-cost neural approximator. *J. Frankl. Inst.* **2022**, *359*, 4938–4958.
6. Wang, X.; Niu, B.; Zhao, X.; et al. Command-filtered adaptive fuzzy finite-time tracking control algorithm for flexible robotic manipulator: A singularity-free approach. *IEEE Trans. Fuzzy Syst.* **2023**, *32*, 409–419.
7. Gao, J.; Tan, Z.; Li, L.; et al. A novel finite-time non-singular robust control for robotic manipulators. *Chaos Solitons Fractals* **2025**, *194*, 116266.
8. Zheng, S.; Zha, Y.; Ahn, C.K.; et al. Constrained Finite-Time Output Regulation for Robot Manipulators With Control Input Delay. *IEEE/ASME Trans. Mechatron.* **2025**, *30*, 1–13.
9. Hu, J.; Zhang, X.; Zhang, D.; et al. Finite-time adaptive super-twisting sliding mode control for autonomous robotic manipulators with actuator faults. *ISA Trans.* **2024**, *144*, 342–351.
10. Chu, Y.; Han, X.; Rakkiyappan, R. Finite-time lag synchronization for two-layer complex networks with impulsive effects. *Math. Model. Control.* **2024**, *4*, 71–85.
11. Polyakov, A. Nonlinear feedback design for fixed-time stabilization of linear control systems. *IEEE Trans. Autom. Control.* **2011**, *57*, 2106–2110.
12. Ahmed, S.; Azar, A.T. Adaptive fractional tracking control of robotic manipulator using fixed-time method. *Complex Intell. Syst.* **2024**, *10*, 369–382.
13. Zhang, D.; Hu, J.; Cheng, J.; et al. A novel disturbance observer based fixed-time sliding mode control for robotic manipulators with global fast convergence. *IEEE/CAA J. Autom. Sin.* **2024**, *11*, 661–672.
14. Zhao, B.; Yao, X.; Zheng, W.X. Fixed-time composite anti-disturbance control for flexible-link manipulators based on disturbance observer. *IEEE Trans. Circuits Syst. I Regul. Pap.* **2024**, *71*, 3390–3400.
15. Lai, G.; Zou, S.; Xiao, H.; et al. Fixed-time adaptive fuzzy control with prescribed tracking performances for flexible-joint manipulators. *J. Frankl. Inst.* **2024**, *361*, 106809.
16. Yu, J.; Wu, M.; Ji, J.; et al. Neural network-based region tracking control for a flexible-joint robot manipulator. *J. Comput. Nonlinear Dyn.* **2024**, *19*, 021003.
17. Sánchez-Torres, J.D.; Gómez-Gutiérrez, D.; López, E.; et al. A class of predefined-time stable dynamical systems. *IMA J. Math. Control. Inf.* **2018**, *35*, i1–i29.
18. Jiang, H.; Yang, Y.; Hua, C.; et al. Predefined-Time Composite Fuzzy Adaptive Control for Flexible-Joint Manipulator System With High-Order Fully Actuated Control Approach. *IEEE Trans. Ind. Electron.* **2025**, *72*, 7191–7199.
19. Sai, H.; Xu, Z.; Zhang, E. Adaptive practical predefined-time neural tracking control for multi-joint uncertain robotic manipulators with input saturation. *Neural Comput. Appl.* **2023**, *35*, 20423–20440.
20. Fan, Y.; Zhan, H.; Li, Y.; et al. A Predefined Time Constrained Adaptive Fuzzy Control Method With Singularity-Free Switching for Uncertain Robots. *IEEE Trans. Fuzzy Syst.* **2024**, *32*, 2650–2662.
21. Wang, J.; Zhao, W.; Cao, J.; et al. Reinforcement Learning-Based Predefined-Time Tracking Control for Nonlinear Systems Under Identifier–Critic–Actor Structure. *IEEE Trans. Cybern.* **2024**, *54*, 6345–6357.
22. Shen, H.; Zhao, W.; Cao, J.; et al. Predefined-Time Event-Triggered Tracking Control for Nonlinear Servo Systems: A Fuzzy Weight-Based Reinforcement Learning Scheme. *IEEE Trans. Fuzzy Syst.* **2024**, *32*, 4557–4569.
23. Wang, Y.; Wang, X.; Chen, S.; et al. Multi-Station Multi-Robot Welding System Planning and Scheduling Based on STNSGA-D: An Industrial Case Study. *IEEE Trans. Autom. Sci. Eng.* **2024**, *21*, 7465–7479.
24. Zhou, X.; Wang, H.; Tian, Y. Robust adaptive flexible prescribed performance tracking and vibration control for rigid–flexible coupled robotic systems with input quantization. *Nonlinear Dyn.* **2024**, *112*, 1951–1969.
25. Ma, H.; Zhou, Q.; Li, H.; et al. Adaptive prescribed performance control of a flexible-joint robotic manipulator with dynamic uncertainties. *IEEE Trans. Cybern.* **2021**, *52*, 12905–12915.
26. Sun, P.; Li, S.; Zhu, B.; et al. Vision-based finite-time prescribed performance control for uncooperative UAV target-tracking subject to field of view constraints. *ISA Trans.* **2024**, *149*, 168–177.
27. Liu, Z.; Zhao, Y.; Zhang, O.; et al. Adaptive fuzzy neural network-based finite time prescribed performance control for uncertain robotic systems with actuator saturation. *Nonlinear Dyn.* **2024**, *112*, 12171–12190.
28. Yang, P.; Su, Y.; Zhang, L. Proximate fixed-time fault-tolerant tracking control for robot manipulators with prescribed performance. *Automatica* **2023**, *157*, 111262.
29. Liu, C.; Zhao, K.; Li, J.; et al. Fuzzy adaptive predefined time control with global prescribed performance for robotic manipulator under unknown disturbance. *IEEE Trans. Syst. Man Cybern. Syst.* **2025**, *55*, 3397–3410.

30. Zhu, B.; Zhang, L.; Niu, B.; et al. Adaptive reinforcement learning for fault-tolerant optimal consensus control of nonlinear canonical multiagent systems with actuator loss of effectiveness. *IEEE Syst. J.* **2024**, *18*, 1681–1692.
31. Ji, N.; Liu, J. Consensus control and vibration suppression for multiple flexible nonlinear Timoshenko manipulators under undirected communication topology. *Commun. Nonlinear Sci. Numer. Simul.* **2024**, *138*, 108200.
32. Zhang, Q.; Zhang, Q.; Liu, J. Adaptive consensus tracking control for robotic manipulators with nonlinear time-varying fault-tolerant actuator and unknown control input directions. *Int. J. Adapt. Control. Signal Process.* **2024**, *38*, 1114–1134.
33. Wang, C.; Zhan, H.; Guo, Q.; et al. Distributed neural fixed-time consensus control of uncertain multiple Euler-Lagrange systems with event-triggered mechanism. *IEEE/ASME Trans. Mechatron.* **2024**, *30*, 1830–1841.
34. Zhao, W.; Li, X.; Liu, Y.; et al. Adaptive Fault Tolerant Consensus Tracking Control for Flexible Manipulators MASs With Input Quantization and Time-Varying Delay. *IEEE Trans. Cybern.* **2025**, *55*, 2597–2607.
35. Stojanović, V. Fault-tolerant control of a hydraulic servo actuator via adaptive dynamic programming. *Math. Model. Control.* **2023**, *3*, 181–191.
36. Guo, X.; Wang, C.; Dong, Z.; et al. Adaptive containment control for heterogeneous MIMO nonlinear multiagent systems with unknown direction actuator faults. *IEEE Trans. Autom. Control.* **2022**, *68*, 5783–5790.
37. Ren, H.; Ma, H.; Li, H.; et al. Adaptive fixed-time control of nonlinear MASs with actuator faults. *IEEE/CAA J. Autom. Sin.* **2023**, *10*, 1252–1262.
38. Zheng, X.; Li, H.; Ahn, C.K.; et al. NN-based fixed-time attitude tracking control for multiple unmanned aerial vehicles with nonlinear faults. *IEEE Trans. Aerosp. Electron. Syst.* **2022**, *59*, 1738–1748.
39. Liang, H.; Chen, L.; Pan, Y.; et al. Fuzzy-based robust precision consensus tracking for uncertain networked systems with cooperative–antagonistic interactions. *IEEE Trans. Fuzzy Syst.* **2022**, *31*, 1362–1376.
40. Yu, J.; Shi, P.; Dong, W.; et al. Observer and command-filter-based adaptive fuzzy output feedback control of uncertain nonlinear systems. *IEEE Trans. Ind. Electron.* **2015**, *62*, 5962–5970.
41. Wang, C.; Lin, Y. Decentralized adaptive tracking control for a class of interconnected nonlinear time-varying systems. *Automatica* **2015**, *54*, 16–24.
42. Yu, W.; Ren, W.; Zheng, W.X.; et al. Distributed control gains design for consensus in multi-agent systems with second-order nonlinear dynamics. *Automatica* **2013**, *49*, 2107–2115.
43. Zhang, H.; Lewis, F.L.; Qu, Z. Lyapunov, Adaptive, and Optimal Design Techniques for Cooperative Systems on Directed Communication Graphs. *IEEE Trans. Ind. Electron.* **2012**, *59*, 3026–3041.
44. Farrell, J.A.; Polycarpou, M.; Sharma, M.; et al. Command Filtered Backstepping. *IEEE Trans. Autom. Control.* **2009**, *54*, 1391–1395.
45. He, W.; Huang, H.; Ge, S.S. Adaptive neural network control of a robotic manipulator with time-varying output constraints. *IEEE Trans. Cybern.* **2017**, *47*, 3136–3147.
46. Huang, A.C.; Chen, Y.C. Adaptive sliding control for single-link flexible-joint robot with mismatched uncertainties. *IEEE Trans. Control. Syst. Technol.* **2004**, *12*, 770–775.